2 Cosmic ray interactions

This book is not a book on high energy physics and particle interactions. We have, however, to give the reader some information on the structure of matter and the interactions between its building blocks, because these are necessary for the understanding of the phenomena of cosmic ray acceleration, propagation in the Universe, and detection.

This chapter gives a simple introduction to our understanding of the structure of matter and of the different interactions that cosmic rays undergo in their propagation from their sources to us. The description of the interactions is brief and biased toward higher energy particles, with an energy of about 1 GeV and higher, which are the main subject of our interest. Three types of interactions are discussed:

- electromagnetic interactions of charged particles, which in are mostly important for the propagation of electrons and photons;
- inelastic hadronic interactions, that are important for the production of secondary particle fluxes;
- nuclear interactions, when heavier nuclei are split into lighter ones, that are mostly important for changes of the chemical and isotopic composition of accelerated cosmic ray nuclei.

We will not discuss the weak interactions in this section. Discussion and formulae for the interactions of neutrinos will be given in Sect. 7.2.1.

2.1 Components and structure of matter

The progress in understanding the structure of matter is intimately and naturally linked to the exploration of smaller and smaller dimension. Rutherford's experiments revealed the existence of the atomic nucleus which takes up a very small fraction of the volume of the atom. Nuclei consist of their components, protons (p) and neutrons (n). The electrons (e^-) are negatively charged particles that orbit the positively charged nucleus to complete the atom.

With the exceptionally rapid development of the experimental particle physics in the last fifty years the number of such 'elementary' particles became very large. The last issue of the *Review of Particle Properties* [11], that keeps

track of all results in the field, lists 143 particles the existence of which is firmly established and whose properties are well known. Most of these particles are not stable. They decay with a very short lifetime. The long-living π^+ decays in 0.026 μs and most other lifetimes are shorter by many orders of magnitude. There are also as many particle 'candidates', the properties of which are not well known and which do not satisfy the conditions for fully established 'elementary' particles.

A few of these particles, such as the electron and electron neutrino (ν_e) are truly elementary, i.e. they are indeed among the building blocks of matter. Both the electron and the neutrino are *leptons*. Others, the *hadrons*, are combinations of smaller blocks, *quarks*, which have never been observed individually, in isolation. Their properties have been derived from the properties of the hadrons they build up because of the conservation of the quantum numbers that these particles carry. A third type of particles is called gauge bosons. These carry the forces between the hadrons and the leptons.

Table 2.1 gives information about the properties of some of the quarks and leptons. Each quark and lepton has its antiparticle. A proton consists of

Table 2.1. Basic building blocks of matter.

Name	Baryon number	Lepton number	Charge
Quarks:			
up (u)	1/3	0	2/3
down (d)	1/3	0	−1/3
Leptons:			
electron (e^-)	0	1	−1
electron neutrino (ν_e)	0	1	0

two up quarks and one down quark. Its structure is *uud*. Consequently it has a baryon number of 1 (1/3 + 1/3 + 1/3) and charge +1 (2/3 + 2/3 −1/3). All charges are measured in units of the electron charge. A neutron consists of one up quark and two down quarks (*udd*). It is neutral (2/3 − 1/3 − 1/3) and has a baryon number 1. The antiparticle of the proton, the antiproton consists of $\bar{u}\bar{u}\bar{d}$. It has a charge of -1 and baryon number −1. All baryons are *strongly* interacting particles. Other hadrons, which also interact strongly, are the mesons. Mesons consist of a quark–antiquark combination. The positive pion π^+ is a ($u\bar{d}$) combination and has a charge of 1 (2/3 −(−1/3)) and baryon number 0 (1/3 − 1/3).

Quarks have also an additional quantum number specific to them, *color*, which allows the combinations of identical quarks, which otherwise would have been forbidden by Fermi's statistics. The classical example for that is

the doubly charged baryon Δ^{++} which consists of three up quarks (uuu) of different colors.

2.1.1 Strong, electromagnetic and weak interactions

The particles shown in Table 2.1 represent only one of the three families of quarks and leptons. Table 2.2 gives the names of all quarks and leptons and the types of their interactions. All charged particles have electromagnetic

Table 2.2. Quarks, leptons, interactions they participate in, and the force carriers.

Name	The three families			Interactions	Gauge boson
Quarks	u (up)	c (charm)	t (top)	strong &	g
	d (down)	s (strange)	b (beauty)	EM	γ
Leptons	e (electron)	μ (muon)	τ (tau)	EM &	γ
	ν_e	ν_μ	ν_τ	weak	$W^\pm, Z$

interactions. Hadrons have also strong interactions and neutral leptons have only weak interactions. These three types of interactions reflect the strength and extension of the corresponding forces. The strong force has a short range of the order of the radius of a proton (1 fm = 10^{-13} cm) and strength α_s of 1. The force is carried by gluons (g). The electromagnetic force is carried by γ-rays and its coupling constant α has strength lower by two orders of magnitude. The weak force is carried by the intermediate vector bosons $W^\pm$ and the neutral Z and has a coupling α_W of the order of $10^{-6}\alpha_s$.

These features are also reflected in the corresponding particle decays. Weak decays, like $\pi^+ \rightarrow \mu^+\nu_\mu$ have lifetimes in excess of 10^{-12} seconds. Note the conservation of the quantum numbers in the decay. The sum of the lepton numbers of the decay products is 0, as is that of the parent π^+. Electromagnetic decays ($\pi^0 \rightarrow \gamma\gamma$) have lifetimes shorter than 10^{-16} s, while decays guided by the strong force have lifetimes of the order of 10^{-23} s.

2.1.2 Units of energy and interaction strength

The basic unit of energy in particle physics and cosmic ray physics is the electronvolt (eV). This is the kinetic energy gained by an electron by passing through a potential difference of 1 V. Different appropriate energy measures are obtained by scaling the eV in threefold order of magnitude units, i.e. a kiloelectronvolt (KeV) is 10^3 eV, megaelectronvolt (MeV) is 10^6 eV, (giga) GeV = 10^9 eV, (tera) TeV = 10^{12} eV, (peta) PeV = 10^{15} eV, (eta) EeV = 10^{18} eV and (zeta) ZeV = 10^{21} eV. The total particle energy and the kinetic

energy $E_k = E - mc^2$ are measured in the same units. Particle momenta $p = (E^2 - m^2c^4)^{1/2}$ are measured in eV/c.

The interaction strength is measured by the interaction cross-section σ, which is expressed in units of area. The basic unit is the barn = 10^{-24} cm^2. Common units are the millibarn, 1 mb = 10^{-3} b and the microbarn, 1 μb = 10^{-6} b. Cross-sections are usually given per one nucleon (or nucleus) of target. If a particle has interaction cross-section of $\sigma = 1$ mb, its mean free path in a medium of nucleon density $\rho = 10^3$ cm^{-3} is $\lambda = (\sigma\rho)^{-1} = 10^{24}$ cm. If the density ρ is in terms of g/cm^3 then the mean free path is calculated in terms of the column density g/cm^2, i.e. $\lambda = [(N_A/A)\rho\sigma]^{-1}$ g/cm^2, where N_A is Avogadro's number and A is the mass number of the target.

Other quantities that we will use soon are the particle Lorentz factor $\gamma = E_{tot}/mc^2$ that is the ratio of the total particle energy and its velocity $\beta = v/c$ in terms of the speed of light. These quantities are related in the following way:

$$\gamma = \frac{1}{\sqrt{1-\beta^2}}$$

2.2 Electromagnetic processes in matter

Most of the information given in this section is directly applicable only for electrons. Later, in Chap. 7 we discuss the electromagnetic interactions and the energy loss of muons.

2.2.1 Coulomb scattering

The basis of all elecromagnetic interactions is the Coulomb scattering between electric charges. The force between two point charges q_1 and q_2 at distance R from each other is

$$F = \frac{q_1 q_2}{R^2}\boldsymbol{n}\,, \tag{2.1}$$

where $\boldsymbol{n}$ is the unit vector from one of the charges to the other.

Experimentally this process was studied by Rutherford in which he discovered the structure of the atom [12]. Rutherford bombarded heavy nuclei with α particles (He nuclei) and measured the angular deflection of the projectile nuclei.

In the Coulomb field the particle trajectory changes. The deflection angle ϑ depends on the impact parameter b between the two charges and the velocity and mass of the particles that carry them. The impact parameter is the closest distance between the two particles with charges q_1 and q_2. The deflection (scattering) angle is

$$\tan\frac{\vartheta}{2} = \frac{zZe^2}{Mv^2b}\,. \tag{2.2}$$

Equation (2.2) expresses the charges in terms of the charge of the electron e. In the case of a projectile electron with charge $z = 1$ one can write the differential cross-section for scattering as

$$\frac{d\sigma}{d\Omega} = \frac{b}{\sin\vartheta}\frac{db}{d\vartheta} = \frac{Z^2}{4}r_e^2 sin^{-2}\frac{\vartheta}{2}, \tag{2.3}$$

where $r_e = e^2/(m_e c^2)$ is the *classical* radius of the electron and Z is the charge of the medium.

The fact that the electrons change their direction suggests that there is transfer of energy between the two particles. This is expressed through the momentum transfer in terms of the momentum of the projectile particle, which here is an electron. The momentum transfer q is related to the electron momentum before the scattering p and the scattering angle ϑ as

$$q = 2p\sin\frac{\vartheta}{2}. \tag{2.4}$$

There are two consequences from the scattering: the projectile particle changes its direction and its energy is changed in the scattering process.

The formulae above are strictly valid for point-like charges moving with nonrelativistic velocity. Several corrections have to be introduced for relativistic particles and for more realistic scattering conditions.

The correction for relativistic particles, that was introduced by Mott, adds the term $(1 - \beta^2\sin^2\frac{\vartheta}{2})$ to the differential cross-section in (2.3).

Another correction is needed to account for the size of the target nucleus. This is the nuclear formfactor, that accounts for the distribution of charge inside the nucleus.

A third important one is for the screening of the nuclear field by the atomic electrons. The basic correction for screening is in the form $(1 + \frac{1}{Za})^{-2}$, where the screening radius a is defined as the exponent of the potential decrease with distance. The screening radius is often approximated as $a = (\hbar^2/me^2)Z^{-1/3}$.

2.2.2 Ionization loss

Charged particles traveling through matter lose energy on excitation and ionization of its atoms. The energy loss per unit of column depth (in units of MeV per g/cm^2) is:

$$\frac{dE}{dx} = -\frac{N_A Z}{A}\frac{2\pi(ze^2)^2}{Mv^2}\left[\ln\frac{2Mv^2\gamma^2 W}{I^2} - 2\beta^2\right], \tag{2.5}$$

where Z is the atomic number of the medium, A is its mass number and I is its average ionization potential. N_A is Avogadro's number. ze is the charge of the the particle, v is its velocity, and M - its mass. γ and β characterize

particle energy and momentum. This expression is obtained by Hayakawa [3] by integrating the formulae of Bethe [13] and Bloch [14] to the maximum energy loss W. The ionization loss is thus proportional to a constant L that includes the charge and atomic number of the medium.

$$L \equiv \frac{2\pi N_A Z}{A}\left(\frac{e^2}{mc^2}\right)^2 mc^2 = 0.0765\left(\frac{2Z}{A}\right) \text{ MeV(g/cm}^2)^{-1} . \quad (2.6)$$

In rarefied media the ionization energy loss increases logarithmically with the particle energy. In (2.5) this is expressed through the γ^2 term. In denser media this increase is suppressed (the density effect), which is accounted for by introducing the term $-\delta$ in (2.5). The energy loss on ionization can then be written in a simplified form as

$$\frac{dE}{dx} = -L\frac{Z^2}{\beta^2}\left(B + 0.69 + 2\ln\gamma\beta + \ln W - 2\beta^2 - \delta\right) \text{ MeV(g/cm}^2)^{-1} , \quad (2.7)$$

where $B \equiv \ln(mc^2/I^2)$, $W \simeq E/2$ and $\delta = 2\ln\gamma\beta$ plus a correction C depending on the particle energy and on the properties of the medium. The $2\ln\gamma\beta$ term compensates for the logarithmic increase of the ionization loss. The parameters guiding the ionization energy loss including the density effect are given in Table 2.3 for particles with momenta $\gg M$ as calculated by Sternheimer [15]. C values in Table 2.3 are only correct at high energy when the ionization loss is almost constant. The low energy values can be found in Hayakawa's book [3] or in the original paper. We give values for a sample of materials, which are important for cosmic ray propagation in the interstellar medium (H, He), in the atmosphere (N, O), and in particle detectors (C, Fe).

Table 2.3. Parameters guiding the energy loss on ionization in different media [3].

Element	I, eV	L	B	C
Hydrogen	21.8	0.152	21.07	−9.50
Helium	44.0	0.077	19.39	−2.13
Carbon	77.8	0.077	18.25	−3.22
Nitrogen	90.9	0.077	17.94	−10.68
Oxygen	104	0.077	17.67	−10.80
Iron	286	0.072	15.32	−4.62

Equation (2.7) gives the average energy loss on ionization. In fact, the energy loss has significant fluctuations, especially when the thickness of the target is small.

2.2.3 Cherenkov light

A small fraction of the energy loss is emitted in the form of Cherenkov radiation. The name is after its discoverer, P. Cherenkov. Cherenkov light is emitted when a particle moves in a medium with velocity βc greater than the phase velocity of the light c/n, where n is the refraction index of the medium.

This requirement sets a threshold energy for the emission of Cherenkov light that depends on the value of the refraction index. The refraction index of air at sea level is $n = 1.0003$ and the threshold energy is $E_{thr} > m\sqrt{1 - 1/n^2}$ (m is the particle mass) ~ 21 MeV for electrons. The refraction index in water is 1.33 which gives much lower threshold energy, about 1 MeV for electrons.

The Cherenkov light is emitted on a cone around the particle trajectory. The cone opening angle is

$$\cos\theta = \frac{1}{\beta n} + q \,, \tag{2.8}$$

where q is a quantum correction factor with small practical importance. The maximum opening angle is achieved at high energy when $\beta = 1$ and $\cos\theta$ is inversely proportional to the refraction index of the medium.

The intensity of the radiation per unit pathlength is proportional to the square of the particle charge and is

$$dN/dL = z^2 \frac{\alpha}{\hbar c}\left[1 - \frac{1}{\beta^2 n^2}\right] \,, \tag{2.9}$$

where $\alpha(\hbar c)^{-1} = 370\ \mathrm{eV}^{-1}\,\mathrm{cm}^{-1}$. The second factor in (2.9) introduces an energy dependence in the threshold energy range. The wavelength distribution of the emitted Cherenkov light is proportional to λ^{-2} and is distributed in the visible and UV range.

2.2.4 Compton scattering

The process in which photons interact with the atomic electrons and transfer a fraction of their energy to the electrons is the Compton scattering. The differential cross-section for Compton scattering of a photon of energy k is given by

$$\sigma_C(k, k') = 2\pi r_e^2 \frac{1}{k'}\frac{1}{q}\left[1 + \left(\frac{k'}{k}\right)^2 - \frac{2(q+1)}{q^2} + \frac{1+2q}{q^2}\frac{k'}{k} + \frac{1}{q^2}\frac{k}{k'}\right] \,, \tag{2.10}$$

where k' is the photon energy after the scattering and q is the primary photon energy in units of electron mass – $q \equiv k/mc^2$.

The total Compton scattering cross-section can be integrated from (2.10) to

$$\sigma_C(k) = \frac{\pi r_e^2}{q} \times \left[\left(1 - \frac{2(q+1)}{q^2} \right) \ln(2q+1) + \frac{1}{2} + \frac{4}{q} - \frac{1}{2(2q+1)^2} \right] . \tag{2.11}$$

At low q values, $q \ll 1$, σ_C approaches the Thomson cross-section σ_T ($= 8\pi r_e^2/3 = 665$ mb) and decreases with increasing energy. For k much greater than the electron mass the total cross-section is well represented by the much simpler formula

$$\sigma_C \simeq \sigma_T \frac{3}{8q} \left(\ln 2q + \frac{1}{2} \right) \tag{2.12}$$

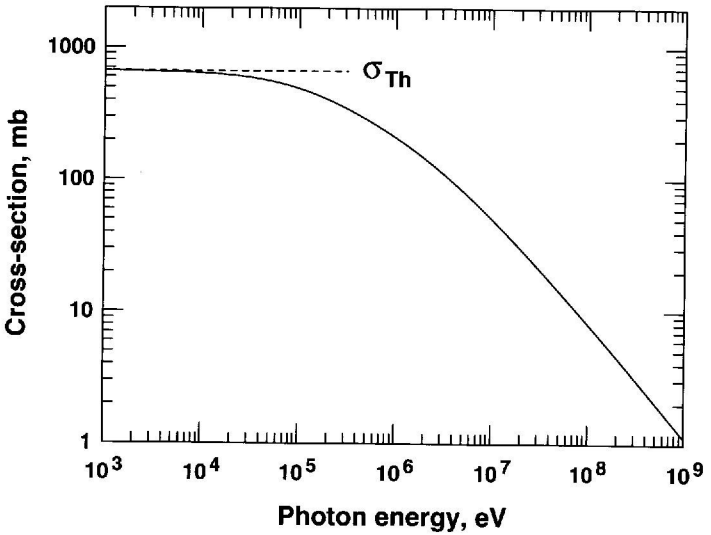

Fig. 2.1. Cross-section for Compton scattering as a function of the photon energy.

The angle between the primary and the secondary photon θ can be expressed as a function of the energies of the photon before and after the scattering.

$$\cos\theta = 1 - \frac{mc^2(k/k' - 1)}{k} , \tag{2.13}$$

which makes Compton scattering a convenient physical base for construction of particle detectors. If the scattered photon and electron are both detected this gives not only the energy of the primary photon but also its direction.

2.2.5 Bremsstrahlung

Charged particles also interact with the electromagnetic field of the atomic nuclei and generate photons. The process is called bremsstrahlung. The energy loss on bremsstrahlung is

$$\frac{dE}{dx} = -\frac{N}{A}\int_0^{E-mc^2} \sigma_{br}(E,k)k\,dk\,, \tag{2.14}$$

where E is the energy of the charged particle and k is the energy of the emitted photon. The bremsstrahlung cross-section σ_{br} for electrons is given as a function of E and k as [16]

$$\sigma_{br} = \frac{4Z^2\alpha r_e^2}{k}F(E,k)\,, \tag{2.15}$$

where $r_e = e^2/\hbar c$ is the classical radius of the electron and α is the fine splitting constant. This cross-section is calculated by Bethe and Heitler [16]. The function $F(E,k)$ depends on the screening parameter ξ, which expresses the screening of the nuclear field by the atomic electrons.

$$\xi \equiv 100Mc^2\frac{k}{E}\frac{1}{E-k}Z^{-1/3}. \tag{2.16}$$

The screening parameter ξ is inversely proportional to the energy of the charged particle and is proportional to the ratio of the electron energy before and after the process. As a function of the ratio of the photon to the electron energy $u = k/E$

$$F(E,k) = \left[4(1-u)/3+u^2\right]\ln Z^{-1/3} + (1-u)/9 \tag{2.17}$$

in the case of vanishing $\xi \simeq 0$, which generally describes interactions of high energy electrons. For large ξ values (in the no screening regime)

$$F(E,k) = \left[4(1-u)/3+u^2\right]\left[\ln\left(\frac{2E}{mc^2}\frac{1-u}{u}\right) - 1/2\right] \tag{2.18}$$

Figure 2.2 shows the form of $F(E,k)$ in these two regimes for electron energy of 100 MeV. The correct representation would be the use of the full screening formula for small k values with the no screening formula for k approaching the electron energy and intermediate formulae in between.

Because of the term $1/k$ the differential cross-section for bremsstrahlung becomes infinite when k approaches 0 and creates the 'infrared catastrophe'. This, however, integrates out when the total energy loss is calculated. For vanishing ξ the energy loss is

$$\frac{dE}{dx} = \frac{4NZ}{A}\alpha r_e^2 E\left[\ln 191Z^{-1/3} + 1/18\right]\,. \tag{2.19}$$

The correction term 1/18 in (2.19) comes from the interactions with the fields of the atomic electrons. The interaction cross-section has the the same form as (2.15) with the Z^2 term replaced by Z. The total bremsstrahlung cross-section is thus proportional to $Z(Z+1)$. This nuclear formfactor varies

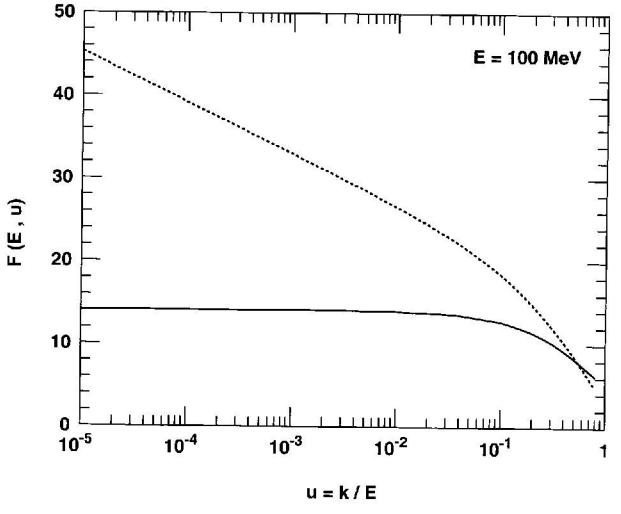

Fig. 2.2. $F(E,k)$ from (2.17) (solid line) and (2.18) (dotted line) for electron energy 100 MeV.

slightly from this general form and for practical reasons is better represented as $Z(Z+1\pm\epsilon)$.

At a certain energy ε_0 the energy loss for bremsstrahlung equals the ionization energy loss. ε_0 is called critical energy and decreases with the charge of the medium Z.

The general form of the energy loss in (2.19) allows the introduction of the radiation length X_0 which gives the average amount of matter for bremsstrahlung energy loss.

$$X_0 \equiv \left[\frac{4NZ(Z+1)}{A}\alpha r_e^2 \ln\left(191Z^{-1/3}\right)\right]^{-1} \tag{2.20}$$

Approximate values for X_0 can be easily calculated with the formula recommended by Hayakawa [3]

$$X_0 \simeq 10^3 \times \frac{A}{6Z(Z+1)}\ \mathrm{g.cm}^{-2}\,. \tag{2.21}$$

More exact values of X_0 and ε_0 in different targets are given in Table 2.4, which is partially extracted from the *Review of Particle Properties* [11].

For mixtures of different elements the radiation length is calculated as a weighted sum of the radiation lengths for the different components

$$\frac{1}{X_0} = \sum_i \frac{w_i}{X_0^i}\,, \tag{2.22}$$

Table 2.4. Radiation lengths and critical energies for the most common elements. The radiation length values are from [11] and the critical energies from [3].

Element	Z	A	X_0, g/cm^2	ε_0, MeV
Hydrogen	1	1.01	61.28	350.
Helium	2	4.00	94.52	250.
Carbon	6	12.01	42.70	79.
Nitrogen	7	14.01	37.99	85.
Oxygen	8	16.00	34.24	75.
Silicon	14	28.09	28.08	37.5
Iron	26	55.85	13.84	20.7

where w_i is the fraction of weight of the component element in the compound mixture. If we assume, for example, that the atmosphere consists only of 25% O nuclei and 75% N nuclei, and has an average atomic weight of 14.5, (2.22) will give us $1/X_0 = 14 \times 0.25/34.24 + 16 \times 0.75/37.99 = 0.02712$ and we obtain $X_0(\text{air}) = 36.9$ g/cm^2. There is still some ambiguity about the exact value of the radiation length in air. The particle data book [11] gives $X_0 = 36.66$ g/cm^2 for sea level and temperature of 20°C. In cosmic ray physics an accepted number is 37.1 g/cm^2.

2.2.6 Creation of electron–positron pairs

It is convenient to discuss the creation of pairs after the bremsstrahlung because physically it is the inverse process. The pair production cross-section σ_{pair} can be calculated by substituting the electron and the positron of the pair for the electron before and after bremsstrahlung. The cross-section then becomes

$$\sigma_{pair}(k,E) = \sigma_{br}(E,k)\frac{E^2}{k^2} = \frac{4Z^2\alpha r_e^2}{k} G(k,E) ,$$

where k is the energy of the primary photon. The function $G(k,E)$ is of the order 1 and can be expressed as a function of the ratio $v = E/k$. E is the energy of one of the members of the pair. The shape of $G(k,E)$ also depends on the screening parameter ξ. For the case of full screening

$$G(k,v) = [1 + 4v(v-1)/3] \ln(191Z^{-1/3}) - v(1-v)/9 . \tag{2.23}$$

For no screening

$$G(k,v) = [1 + 4v(v-1)/3] \times \left[\ln\left(\frac{2k}{mc^2}\right) v(1-v) - 1/2\right] . \tag{2.24}$$

Figure 2.3 shows the function $G(k,v)$ for primary proton energy $k = 100$ MeV in the two extreme cases of full screening and no screening, which at

this energy are very different. It is thus extremely important to use the correct expressions as the incorrect application of the simple equation (2.23) can lead to errors of one order of magnitude.

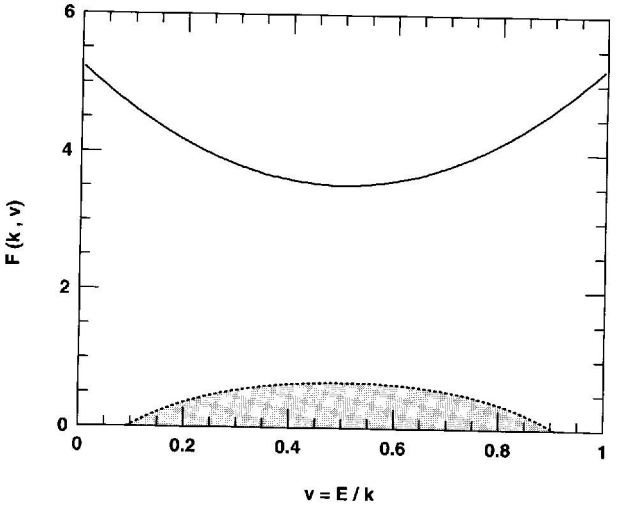

Fig. 2.3. $G(E,k)$ from (2.23) (solid line) and (2.24) (dotted line, shaded areas) for primary photon energy 100 MeV.

The total pair production cross-section can be directly integrated

$$\begin{aligned}\sigma_{pair}(k) &= \int_{mc^2}^{k-mc^2} \sigma_{pp}(k,E)\,dE \\ &= 4Z^2\alpha r_e^2 \frac{\ln(191Z^{-1/3})}{9} - \frac{1}{54}\end{aligned} \tag{2.25}$$

in the case of vanishing ξ. The correction term $1/54$ comes from pair production in the field of the atomic electrons.

2.3 Electromagnetic collisions on magnetic and photon fields

2.3.1 Synchrotron radiation

Synrotron radiation is a very important energy loss process for charged particles in the presence of magnetic fields. In astrophysics it is often called magnetic bremsstrahlung. An electron moving in magnetic field B with an angle θ to the field direction loses energy to synchrotron radiation at a rate

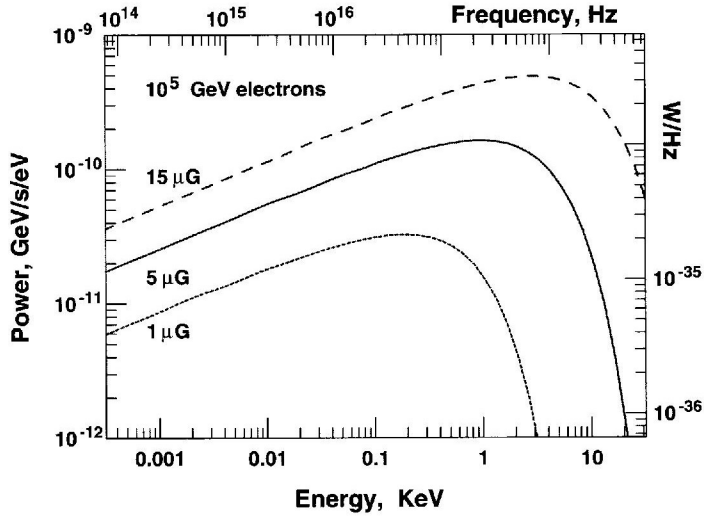

Fig. 2.4. Power spectrum of synchrotron radiation emitted by 10^5 GeV electrons in 1, 5, and 15 μG fields.

$$-\frac{dE}{dt} = 2\sigma_T c\gamma^2 U_B \beta^2 \sin^2\theta \,, \tag{2.26}$$

where β and γ are the velocity and Lorentz factor of the electron, U_B is the energy density of the magnetic field ($= B^2/8\pi$) and σ_T is the Thomson cross-section. Note that the synchrotron energy loss is proportional to the square of the particle Lorentz factor and is thus inversely proportional to the square of the particle mass for the same total energy E_{tot}. A proton loses only $(m_e/m_p)^2 \simeq 3 \times 10^{-7}$ times as much energy as an electron of the same E_{tot}.

For an ensemble of electrons that are scattered randomly in all directions one could calculate the energy loss averaged over all pitch angles, which is

$$\left\langle -\frac{dE}{dt} \right\rangle = \frac{4}{3}\sigma_T c\gamma^2 U_B \tag{2.27}$$

for relativistic electrons with $\beta \simeq 1$. Expressed in particle physics units the average energy loss becomes

$$-\frac{dE}{dt} = 3.79 \times 10^{-6} \left(\frac{B}{\text{gauss}}\right)^2 \left(\frac{E_e}{\text{GeV}}\right)^2 \text{GeV/s} \,. \tag{2.28}$$

The characteristic frequency of the radiated photons is the critical frequency

$$\nu_c = \frac{3}{4\pi}\gamma^2 \frac{eB}{m_e c} \sin\theta = 1.61 \times 10^{13} \left(\frac{B}{\text{gauss}}\right) \left(\frac{E}{\text{GeV}}\right)^2 \text{Hz} \,. \tag{2.29}$$

Expressed as a fraction of the electron energy the critical frequency is proportional to the product of the energy and the magnetic field value $\nu_c/E_e \propto E_e \times B$. The higher the energy and the magnetic field, the harder is the spectrum of the radiated photons.

The emissivity of a relativistic electron of energy E_e averaged over all pitch angles cannot be expressed in a final analytic form and is given by the integral

$$j(E,\nu)\,d\nu \;=\; \frac{\sqrt{3}e^3B}{m_ec^2}\int_0^{\pi} d\theta\,\sin^2\theta/2(\nu/\nu_c)\,d\nu\int_{\nu/\nu_c}^{\infty} K_{5/3}(\eta)\,d\eta\;, \qquad (2.30)$$

where $K_{5/3}$ is the Bessel function of order 5/3. The number spectrum of the synchrotron radiation peaks at $0.29\nu_c$. Figure 2.4 shows the power spectrum of synchrotron radiation of a 10^5 GeV electron in 1, 5 and 15 μG fields. Note the shift of the critical frequency ν_c with the increase of the strength of the magnetic field.

Synchrotron radiation plays a very important role in astrophysics as described in the book [68] of Ginzburg. It is a major contributor to the non-thermal emission spectra of all astrophysical sources in a very wide frequency range stretching from radio waves to X-rays. The physical picture of the synchrotron emission is described in the book of Longair [7] and the full derivation of all relevant formulae is given by Blumenthal & Gould [69].

In spite of the complicated expression for the spectrum of photons radiated by a single electron the spectrum emitted by electrons with a power law distribution is well defined. If the differential power law index of the electron spectrum is α the integral spectral index of their synchrotron emission is $(\alpha - 1)/2$.

2.3.2 Inverse Compton effect

The formulae for Compton effect, equations (2.10) and (2.11), are also applicable to the inverse Compton effect, the interaction when an electron interacts with a photon from an ambient photon field, loses energy and boosts the photon. The formulae can be used when the energy of the primary electron E (which is assumed to be m_ec^2 in (2.10)) and the ambient photon ϵ are used to represent the photon energy in the electron rest frame, i.e.

$$k \;=\; \frac{\epsilon E}{m_ec^2}(1-\beta\cos\theta)\;, \qquad (2.31)$$

where $\cos\theta$ is the angle between the photon and the electron in the photon frame and β is the electron velocity in units of c.

The inverse Compton scattering is a very important process for the production of very high energy γ-rays when accelerated electrons collide with photons of the microwave background radiation of other ambient fields. In the Thomson regime ($\epsilon E \ll (m_ec^2)^2$) the cross-section is approximatelly

σ_T and the average energy of the boosted photon $E_\gamma = \epsilon(E/m_e c^2)^2$. For $\epsilon E \gg (m_e c^2)^2$ the average E_γ approaches the electron energy E. The cross-section is then much smaller.

Using these estimates we can also write the energy loss formulae for the electrons. In the Thomson regime

$$-\frac{dE}{dx} = \sigma_T U \left(\frac{E}{m_e c^2}\right)^2 , \tag{2.32}$$

where U is the energy density of the photon field. In the high energy (Klein–Nishina) regime

$$-\frac{dE}{dx} = \frac{3}{8}\sigma_T U \left(\frac{m_e c^2}{\epsilon}\right)^2 \ln\left(\frac{2\epsilon E}{m_e^2 c^4}\right) . \tag{2.33}$$

An important production mechanism for very high energy γ-rays combines the synchrotron radiation with the inverse Compton effect. High energy electrons first lose energy on synchrotron radiation and then boost the synchrotron photons to TeV by inverse Compton effect.

2.4 Inelastic hadronic interactions below 1000 GeV

This book will deal a lot with the interactions of hadrons in different energy ranges. At high energy these interactions are well understood and fairly well described by the Quantum Chromo Dynamics theory, which is based on the principles outlined in Sect. 2.1. At relatively low energies, though, the theory does not work and we have to rely on the phenomenological description of the particle interactions. This is what we will discuss in this section. Later, in part II, we shall discuss the way interactions are understood in terms of QCD. Let us start with several general definitions.

A particle of mass M that moves with a velocity βc cm/s is fully characterized by a four–vector $\mathbf{p}$. The components of $\mathbf{p}$ are the particle energy E and the particle momentum $\boldsymbol{p}\,(p_x, p_y, p_z)$ – $\mathbf{p}^2 = E^2 - |\boldsymbol{p}|^2 = m^2$. The relative particle velocity $\beta = \boldsymbol{p}/E$ and its Lorentz factor $\gamma = (1 - \beta^2)^{1/2} = E/m$.

It is very convenient to discuss hadronic interactions in the center of mass (CM) system, in which the momenta of the two interaction particles are collinear, have the same magnitude and point in opposite directions. The total CM energy of the interaction, $\sqrt{s}$ is

$$\sqrt{s} = (\mathbf{p}_1 + \mathbf{p}_2)^2 = \left[(E_1 + E_2)^2 - (\boldsymbol{p}_1 - \boldsymbol{p}_2)^2\right]^{1/2} . \tag{2.34}$$

When one of the interacting particles is at rest

$$\sqrt{s} = (m_1^2 + m_2^2 + 2m_2 E_1^{Lab})^{1/2}, \tag{2.35}$$

where E_1^{Lab} is the energy of the incident particle 1 in the rest frame of the particle 2. This is the laboratory (Lab) frame.

An inelastic interaction is by definition such an interaction where at least one new (secondary) particle is created. From (2.34) it follows directly that $\sqrt{s}$ has to be large enough to accommodate the mass of the secondary particle. If two protons collide and produce a neutral pion, $p + p \longrightarrow p + p + \pi^0$, the CM energy has to be larger than $\sqrt{s} > 2m_p + m_\pi = 2.01$ GeV. The minimum energy of the incident proton in the Lab frame is then $E_1 = s/2m_p - m_p = 1.22$ GeV. This is the absolute minimum energy required for the production of a neutral pion in the interactions of two protons.

The cross-section for inelastic interactions depends on the incident particle energy. Figure 2.5 shows the direct data on the pp inelastic cross-section measured in accelerator experiments from the compilation of Ref. [17]. Although the errors in the threshold region are significant, the data show a quick rise to ~ 30 mb in the threshold region between 1 and 2 GeV, and then a smooth logarithmic increase at higher energy. The measurement of the in-

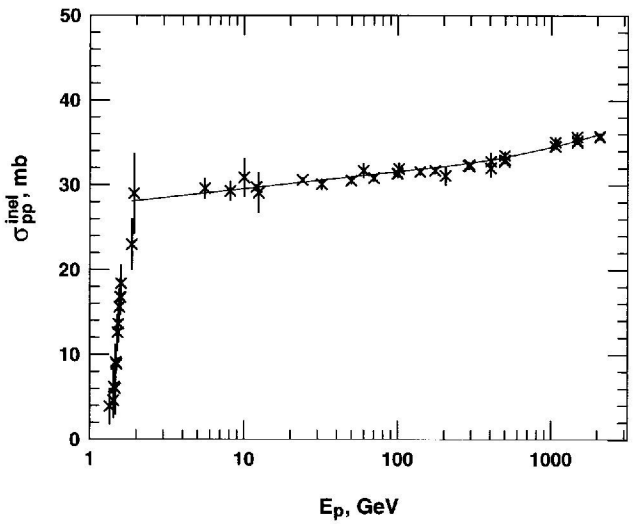

Fig. 2.5. Results from direct accelerator measurements of the pp inelastic cross-section. The data points are from the compilation of Ref. [17] and the line is the fit from Ref. [18].

elastic cross-section are very difficult, because they require detectors with a full 4π coverage of the interaction region. Much more certain estimates are obtained by separate measurements of the total σ_{pp}^{tot} and the elastic σ_{pp}^{el} cross-sections. σ_{pp}^{inel} is the difference between the total and the elastic cross-sections

and its energy dependence is established very well by fits of all available measurements.

Δ resonance. Two-body decays. Lorentz transformation

The threshold energy range in Fig. 2.5 is dominated by the production of resonances. A resonance is a hadronic state with defined quantum numbers and quark content and mass depending on the amount of energy available for its production. The most common (with highest production cross-section) resonance is $\Delta(1232)$ with an average mass of 1.232 GeV and width $\Gamma = 115$ MeV.

The width of the Δ resonance is defined by the elastic cross section of its production in $p\pi$ (or $p\gamma$ collisions. It is described by the Breit–Wigner formula

$$\sigma_\Delta \propto \frac{\Gamma^2/4}{(E - m_\Delta)^2 + \Gamma^2/4} . \tag{2.36}$$

In pp interactions the Breit–Wigner formula reflects the amount of energy available for Δ production in the CM system. The width Γ is defined so that the production cross-section decreases by a factor of 2 at $E = m_\Delta + \Gamma/2$ from its maximum value at $E = m_\Delta$, as shown in Fig. 2.6.

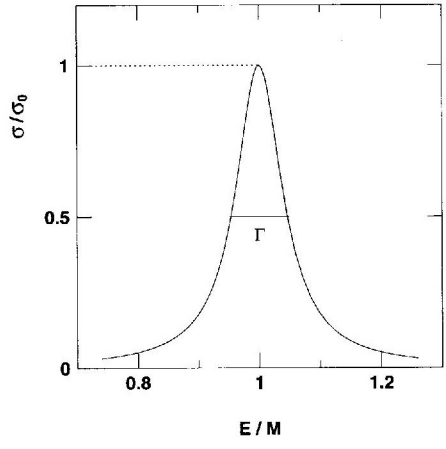

Fig. 2.6. The elastic cross-section for resonance production as a function of the ratio between the incident energy E and the resonance mass M as described by the Breit–Wigner formula.

In a two-body decay the two final state particles share the available energy (the mass of the decaying particle) according to the value of their own mass because their momenta are equal in absolute value. In the decay $M \longrightarrow m_1 + m_2$ $|\boldsymbol{p}_1| = |\boldsymbol{p}_2| = p$, where

$$p = \frac{\left[(M^2 - (m_1 + m_2)^2)(M^2 - (m_1 - m_2)^2)\right]^{1/2}}{2M} . \qquad (2.37)$$

In the frame of the decaying particle the energies $E_{1,2}$ are respectively $E_{1,2} = (M^2 + m_{1,2}^2 - m_{2,1}^2)/2M$. In the case of $\Delta \longrightarrow p + \pi^0$ decay the momenta of both the proton and the π^0 are $p^\Delta = 0.227$ GeV/c and the energies in the Δ frame are $E_p^\Delta = 0.965$ GeV and $E_\pi^\Delta = 0.267$ GeV.

The two decay products will have the same energies and momenta in the center of mass system only if the Δ were stationary in CM. Otherwise the energies and the longitudinal components of the momenta (in the direction of the Δ velocity have to be Lorentz transformed using the Lorentz factor of the Δ in the CM system $\gamma_\Delta = E_\Delta^{CM}/m_\Delta$. The transformation is:

$$E_p^{CM} = \gamma_\Delta(E_p^\Delta + \beta p^\Delta \cos\theta) \quad E_\pi^{CM} = \gamma_\Delta(E_\pi^\Delta - \beta p^\Delta \cos\theta) , \qquad (2.38)$$

where θ is the angle between the proton direction in the Δ frame and the Δ direction in the CM frame. The minus sign in the transformation of the pion energy appears because the proton and the pion move in opposite directions in the Δ frame. The longitudinal momenta $p_\parallel$ are transformed as

$$\begin{aligned} p_{p,\parallel}^{CM} &= = \gamma_\Delta(p^\Delta \cos\theta + \beta E_p^\Delta); \\ p_{\pi,\parallel}^{CM} &= = \gamma_\Delta(-p^\Delta \cos\theta + \beta E_\pi^\Delta) \end{aligned} \qquad (2.39)$$

and the transverse momenta $p_\perp$ (normal to $p_\parallel$) are not changed.

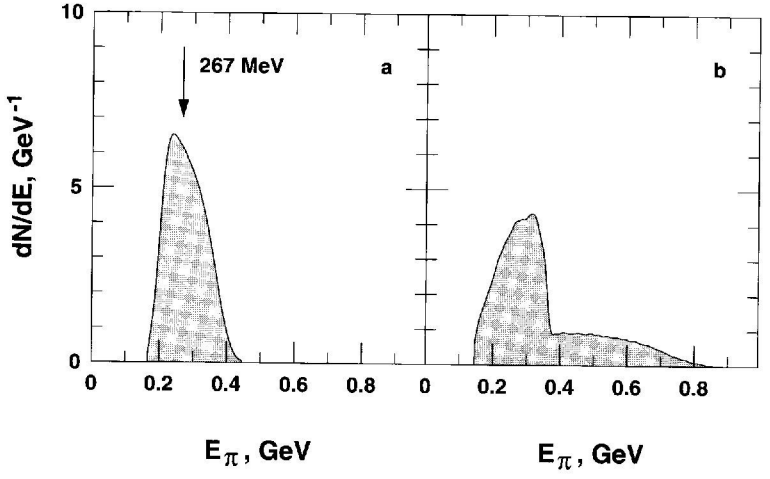

Fig. 2.7. Energy distribution of pions from Δ decay in the CM (a) and the Lab (b) systems. The Δ's are generated in pp collisions of Lab energy of 2 GeV.

Another Lorentz transformation is necessary to obtain the energy of the two decay products in the Lab system. The Lorentz factor of the CM system

in the Lab is $\gamma_{CM} = (E_1^{Lab} + m_2)/\sqrt{s}$. Figure 2.7 shows the energy distributions of pions generated in $\Delta \longrightarrow p + \pi^0$ decays in pp interactions at $E_1^{Lab} = 2$ GeV. The arrow in the left-hand panel shows the pion energy in the Δ frame. The pion energy distribution in the CM frame is generated by the Δ velocity in the CM frame. The distribution in the Lab system is still much wider and shows two different components that are generated by Δ resonances moving forwards and backwards in the CM frame.

$\Delta(1232)$ is the lightest resonance that dominates the inelastic cross-section at its energy threshold. It is followed by a number of heavier resonances the production of which require higher CM energy. Each one of these resonances has lower cross-section than $\Delta(1232)$. The sum of all resonances in the *second resonance region* (heavier than $\Delta(1232)$), however, is at least equally important close to the threshold for inelastic interactions. The masses, widths and decay channels for all identified resonances are listed in the Particle Data Book [11].

2.4.1 Secondary particles spectra, average multiplicity and inelasticity

In the resonance region the multiplicity of the secondary particles in the final state (when all short-lived particles have already decayed) is fixed since every resonance has a well defined set of decays branches. At higher energy, $\sqrt{s} \approx 2.5$ GeV the resonance production is no longer dominant and the interactions are dominated by multiparticle production. The inelastic interaction at this and higher energy are described by a combination of parameters which parametrize the energy spectra and the multiplicity of the secondary particles.

The typical accelerator experiments in this energy range do not measure all secondaries, rather the particles of given type that are emitted with given momentum at certain angle to the direction of the incident particle beam. The general assumption is that the probability for the production of a particle with longitudinal momentum $p_{\parallel}$ and transverse momentum $p_{\perp}$ can be factorized in terms of the two components of the momentum as

$$\frac{d^2\sigma}{dp_{\parallel}dp_{\perp}} = \sigma^{inel} f(p_{\parallel}) \times g(p_{\perp}). \tag{2.40}$$

Experimental data that study the secondary particle production in different (overlapping or complementary) regions of the parameter space could be analyzed together in terms of σ^{inel} and the functions f and g.

A very important hypothesis of the analysis of accelerator data in this energy range is that with increasing energy, when $\sqrt{s}$ becomes significantly higher than the masses on the particles involved in the inelastic interactions, the cross-section σ^{inel} will become constant and the functions f and g will not depend on $\sqrt{s}$. There are different versions of this *scaling* hypothesis.

Feynman scaling, introduced by R. Feynman [19] postulates scaling in terms of $x_F = p^{CM}/(\sqrt{s}/2)$ where $\sqrt{s}/2$ is the maximum momentum that a particle can have in the center of mass system. In terms of x_F the momentum distribution of the secondary mesons in pp collisions have $\frac{1}{x}(1-x_F)^n$ spectrum, with the power n for pions $n_\pi \approx 4$. The $p_\perp$ distribution approaches an energy independent shape with $\langle p_\perp^\pi \rangle = 0.34$ GeV/c.

Another version is that of *radial scaling* [20], which uses the scaling variable $x_R = E^{CM}/(2\sqrt{s})$. Hillas [18] uses the radial scaling hypothesis to parametrize the particle production data in pp collisions at Lab energy from 10 to 2000 GeV in the laboratory system. This parametrization is very useful for the description of cosmic ray collisions. The general form, after a transformation in the Lab system and integration over $p_\perp$ is

$$x\frac{dn}{dx} = f(x) \times H(E)\,, \tag{2.41}$$

where E is measured in the Lab system and $x = E/E_0$, where E_0 is the incident proton energy in the Lab.

For π^+, π^-, and π^0

$$f^\pi(x) = 1.22(1-x)^{3.5} + 0.98\exp(-18x) \tag{2.42}$$

and

$$H^\pi = \left(1 + \frac{0.4}{E - 0.14}\right)^{-1}\,, \tag{2.43}$$

where the energy is in GeV. Similar expressions describe the production of kaons and nucleon–antinucleon ($N\bar{N}$) pairs. The protons in this model have flat x distribution. The average transverse momenta for kaons and for the leading (fastest, most energetic) nucleon in this fit are respectively 0.40 and 0.50 GeV/c.

Equations (2.41) and (2.42) describe very well the experimental data. The agreement is also good for the forward hemisphere after a transformation in the CM system. Since the parametrization is aimed for use in cosmic ray calculations in the Lab, where the particles from the backward CM hemisphere are not essential, the discrepancies in that part of the phase space are not very important. Figure 2.8 shows the x distributions for pions and kaons as fitted by Hillas. Reference [18] also gives the fit to σ_{pp}^{inel} which is shown in Fig. 2.5 with a solid line. The parametrization as a function of the incident proton energy in the Lab is

$$\sigma_{pp}^{inel} = 32.2\left(1 + 0.237\ln\frac{E}{200\,\mathrm{GeV}} + 0.01\ln^2\frac{E}{200\mathrm{GeV}}\,\vartheta\,\frac{E}{200\mathrm{GeV}}\right)\ \mathrm{mb}\,, \tag{2.44}$$

where ϑ is the Heaviside function. As can be seen in Fig. 2.5, equation (2.44) provides a very good fit to the measured cross-section above $\sqrt{s} = 2$ GeV.

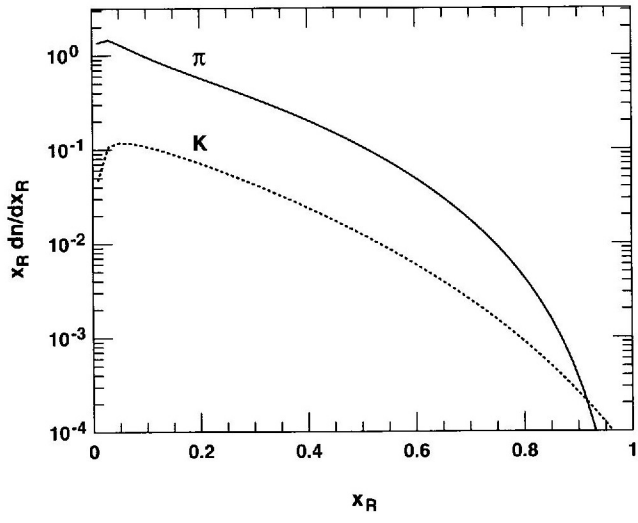

Fig. 2.8. Energy spectra of the secondary pions (solid line) and kaons (dots) calculated for incident proton energy of 100 GeV from the parametrizations of Ref. [18] in terms of the laboratory radial scaling parameter x_R (see (2.42) and (2.43)).

Integrating from 0 to 1 the expression $f(x) \times H(E)\,dx/x$ gives the average multiplicity of pions produced in pp interactions. Equations (2.42) and (2.43) do not work exactly (because they are intended for use in cosmic ray experiments and do not represent exactly the backward hemisphere) but similar parametrizations in the CM system give very good representations of the observed particle multiplicity. The experimental data on the multiplicity of secondary particles is summarized in several papers [21] and [22] that give parametrizations of the multiplicity of charged secondary particles as a function of the interaction energy. Albini et al. [21] express the charged multiplicity as

$$\langle n^{ch} \rangle = 1.17 + 0.30 \log s + 0.13 \log^2 s\,, \tag{2.45}$$

while Thome et al. [22] write

$$\langle n^{ch} \rangle = 0.88 + 0.44 \log s + 0.118 \log^2 s. \tag{2.46}$$

The two expressions agree very well in the region of the fits, as could be seen in Fig. 2.9. The figure also shows the average multiplicity of charged pions and kaons as given by Antinucci et al. [23], who parametrized the energy dependence of the multiplicity of different types of secondaries. Since the measurements of different secondaries have not been made in the same energy ranges, the sum of all secondaries from Ref. [23] only roughly agrees with the expressions 2.45 and 2.46.

A very important general parameter of the inelastic collisions is the coefficient of inelasticity K_{inel}. By definition this is the fraction of the primary

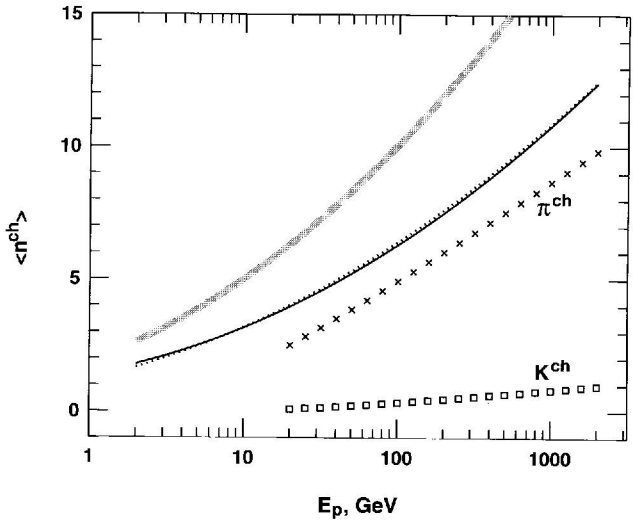

Fig. 2.9. Average charged multiplicity as parametrized by Ref. [21] (solid line) and by Ref. [22] (dotted line). The symbols show the average multiplicity of charged pions and kaons from the summary of Antinucci et al [23]. The thick lighter curve shows the average charge multiplicity in proton interactions on air nuclei.

energy E that a particle has conserved after an inelastic interaction, i.e. $K_{inel} = 1. - \sum_i E_s^i/E$, where the sum is over all secondary particles i generated in the interaction. In the Hillas model the leading secondary nucleons (which are fragments of the primary nucleons) have a flat distribution and $K_{inel} = 0.5$. This is an accepted number for pp interactions at moderate energies. There is a decrease of K_{inel} at $\sqrt{s}$ values above $\sim$ 50 GeV. The distribution of leading nucleons is, however, not flat. About 18% of the inelastic cross-section is *diffractive* where the leading nucleon takes most of the energy and very few secondaries are produced. One half of the diffractive interactions are diffractions of the target nucleon. In the Lab system such interactions could be considered as non-diffractive. For cosmic ray purposes the diffractive cross-section is 9% of the total inelastic cross-section. Summing over the distribution of the leading nucleons one again obtains $K_{inel} \simeq 0.5$. Sometimes the elasticity coefficient $K_{el} = 1 - K_{inel}$ is used instead of K_{inel}.

2.4.2 Kinematic variables and invariant cross-section

Experimental data taken at a certain angle with respect to the incident particle beam are represented as functions of a pair of variables that express the longitudinal and transverse characteristics of the detected particles. Such sets could be $(p_{\parallel}^{Lab}, \vartheta^{Lab})$*, which is used in counter experiments, the already in-*

troduced Feynman scaling variable $x_F = 2_{\parallel}/\sqrt{s}$ *and* $p_\perp^2$ *(or* $p_{\parallel}^{Lab}$, $p_\perp^2$*) or a combination of those, the particle rapidity* y*. The rapidity is defined as:*

$$y = \frac{1}{2}\ln\frac{E+p_{\parallel}}{E-p_{\parallel}} = \ln\frac{E+p_{\parallel}}{m_\perp}\,, \tag{2.47}$$

where $m_\perp = \sqrt{m^2+p_\perp^2}$*. Rapidity is very easy to transform from one system to another because the transformation only adds a constant to the rapidity value, i.e.* $y^{Lab} = y^{CM} + \zeta$*, where* $\zeta = \ln\sqrt{s}/m_p$ *for pp collisions. The energy and longitudinal momentum of a particle in any frame are expressed as a function of the rapidity as*

$$E = m_\perp \cosh y;\; p_{\parallel} = m_\perp \sinh y. \tag{2.48}$$

The maximum rapidity of a particle in the CM system is $y_{max}^{CM} = \ln\sqrt{s}/m$*. When the momenta of the secondary particle are unknown and only the angle* ϑ *can be observed the kinematic variable is the pseudo rapidity* $\eta = -\ln\tan\vartheta/2$*. The pseudorapidity* $\eta \simeq y$ *for momenta much greater than the particle mass and angles* $\vartheta \gg 1/\gamma$*, where* γ *is the particle Lorentz factor. It is closely related to the old cosmic rays variable* $\log_{10}\tan\vartheta^{Lab}$*.*

The production of particles with certain longitudinal and transverse characteristics is usually expressed in terms of the Lorentz invariant cross-section $2E\frac{d\sigma}{d^3p}$*. In terms of the other kinematic variables the invariant cross-section is written as*

$$\begin{aligned} 2E\frac{d\sigma}{d^3p} &= \frac{2E}{\pi}\frac{d\sigma}{p_{\parallel}dp_\perp^2} \\ &= \frac{2x_0}{\pi}\frac{d\sigma}{dx dp_\perp^2} \text{ with } x_0 = \sqrt{x^2+2m_\perp/\sqrt{s}} \\ &= \frac{\pi}{2}\frac{d\sigma}{dy\,dp_\perp^2} \\ &= \frac{2E}{p^2}\frac{d\sigma}{dp\,d\Omega}. \end{aligned} \tag{2.49}$$

2.5 Nuclear fragmentation

Nuclei are complicated systems of protons and neutrons that are held together by a multitude of forces. The simplest model of a nucleus, the liquid drop model, treats it as a fluid consisting of these nucleons. It is easy to derive the nuclear binding energy E_b of a nucleus of mass A consisting of N neutrons and Z protons in this model. It is given by the difference between the masses of the constituent nucleons and the nucleus itself.

$$\frac{E_b}{c^2} = \Delta M_A = Zm_p + Nm_n - M_A \tag{2.50}$$

The order of magnitude for the average binding energy is 20 MeV per nucleon. Rachen [24] has represented the semi-empirical Weizsäcker mass formula in terms of the nuclear mass A in the liquid drop model for stable nuclei as

$$E_b(A) = A\left[15.8 - 18.3A^{-1/3} - 0.18A^{2/3} + 1.3 \times 10^{-3}A^{4/3} - 6.4 \times 10^{-6}A^2\right] \tag{2.51}$$

From energy conservation one can also calculate what is the energy required to separate a fragment F containing N_F neutrons and Z_F protons from the nucleus A. This is the separation energy equal to the difference in the binding energy of the original nucleus and the two nuclei in the final state.

$$E_s = E_b(N, Z) - E_b(N_F, Z_F) - E_b(N - N_F, Z - Z_F) \tag{2.52}$$

This energy would be the threshold for the reaction $A \to F$ if the protons did not carry electric charge. The charge of the nucleus decreases E_s by an amount E_s^C, which represent the Coulomb barrier.

$$E_s^C \simeq \frac{Z_F(Z - Z_F)}{(A - F)^{1/3}} \tag{2.53}$$

The term in the denominator is the estimate of the radius of the remnant nucleus, after separating F.

The total energy needed to separate the fragment from the nucleus will be $E_s^{tot} = E_s - E_s^C$. This gives some ground rules for estimating the probability for separating single nucleons from a nucleus. That probability depends strongly on E_s^C because E_s is the same if we use the parametrization 2.51, which is based on the average charge of stable nuclei of mass A. It is generally easier to separate a proton from a nucleus than it is to separate a neutron. This is indeed true for relatively light nuclei with equal number of protons and neutrons, but not for heavy nuclei with many more neutrons than protons because the nucleus as a whole is positively charged.

The process is much more complicated than our simple treatment here. The account for the quantum effects show that the threshold energy is actually lower because of tunneling. A detailed treatment should also include the Fermi motion of the nucleons inside the nucleus.

Generally one could distinguish two types of nucleons in a nuclear collision. The 'participants' have direct collisions with nucleons from the other colliding nucleus. The 'spectators' are the rest of the nucleons, which do not participate directly in the collision. They are, however, also excited by the collision gaining energy from collisions with some of the participant nucleons and from the surface deformation of the 'pre–fragment' nucleus which contains all spectators. The 'pre–fragment' nucleus relaxes by evaporation in

smaller fragments. For heavy nuclei ($A > 60$) an empirical distribution exists for the masses of the fragments in the final state. The distribution is [25]

$$P(x) \propto 0.1/x^{2.5} + \exp(3.7x) , \tag{2.54}$$

where x is the ratio of the fragment mass to the mass of the original nucleus. $P(x)$ has a minimum at about $x = 1/3$. The branch of the distribution left of that minimum is called multifragmentation, because the parent nucleus fragments in many light fragments including numerous constituent nucleons. The part of the distribution above $x = 1/3$ describes the spallation, i.e. fragmentation processes which result in a large fragment and the emission of several constituent nucleons. Figure 2.10 shows the distribution of fragments for iron nuclei interacting on carbon target.

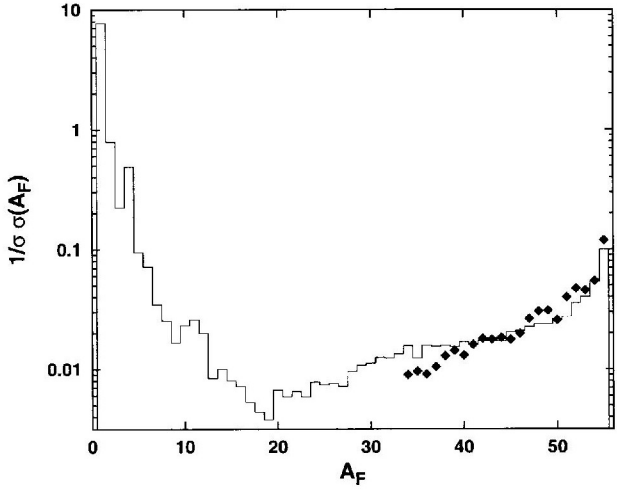

Fig. 2.10. Mass distribution of the fragments in Fe collisions on C target. The data are from Ref. [26] and the calculation is from Ref. [27].

The partial cross-section for the fragmentation of nucleus A into nucleus of mass A' could be written as $\sigma_{A\to A'} = a\sigma_0 P(A'/A)$ and is called the mass changing cross-section. The normalization is chosen so that the sum over all fragmentation probabilities P_j equals 1. The total mass changing cross-section for a nucleus of mass A at a given energy is σ_0. The charge changing cross-sections are similarly defined. The total cross-sections are proportional to $A^{2/3}$. The total cross-sections as well as the particle cross-section have very strong energy dependence at kinetic energies comparable to the nucleon mass. At higher energy, ~5 GeV per nucleon the cross-sections saturate and become nearly constant. Silberberg and collaborators [28] give the following parametrizations for the total mass changing cross-section as a function of the nuclear mass

$$\sigma = 45A^{0.7}\left[1 + 0.016\sin\left(5.3 - 2.63\ln A\right)\right]\text{mb}. \tag{2.55}$$

The energy dependence of the cross-sections are defined with respect to the constant cross-section at energies above several GeV/nucleon. The parametrizations as a function of the kinetic energy per nucleon is

$$\sigma(E_k) = \sigma_{HE}\left[1 - 0.62\exp(-E_k/200\text{MeV}) \times \sin\left(10.9(E_k/\text{MeV})^{-0.28}\right)\right], \tag{2.56}$$

where σ_{HE} is the constant high energy value. The cross-sections peak in the region of the giant resonance, about 20 MeV/nucleon, reaching 60% above the high energy value, then reach a minimum at energy about 200 MeV and then slowly grow to reach the constant high energy value at about $E_k = 2$ GeV.

Nuclear fragmentation is a very complicated process which cannot be fully described in analytic terms. We have to rely on measurements of the partial and the total cross-sections. The data set of such measurements is large but still inadequate for the description of all possible fragmentation channels of all existing nuclei. It is therefore important to interpolate between different measured cross-sections using basic nuclear physics knowledge and the trends observed in the data samples. A very valuable compilation and interpolation procedure was developed by Silberberg & Tsao [29], which is widely used in studies of the cosmic ray propagation. More recently there have been extensive new cross-section measurements [30, 31] that will help significantly in the understanding of the formation of the chemical composition of the cosmic rays.